# Enhanced Fault Location Method for Shunt Capacitor Banks

H. Jouybari-Moghaddam
Department of Electrical
and Computer Engineering
Western University, London, ON, Canada
hjouybar@uwo.ca

Tarlochan Sidhu
The University of Ontario
Institute of Technology
Oshawa, ON, Canada
Tarlochan.Sidhu@uoit.ca

Palak Parikh and Ilia Voloh
GE Grid Solutions
Markham, ON, Canada
Palak.Parikh@ge.com
Ilia.Voloh@ge.com

***Abstract*—High Voltage Shunt Capacitor Banks (SCBs) are the most economical and critical components in the power system, providing reactive power and voltage support. Over temperature, over voltages, manufacturing defects can cause internal failures of capacitor elements. With todays sensitive protection available in numerical relays capacitor elements failure will be detected and capacitor bank will be taken out of service. But determining the phase and section in which capacitor elements have failed is important for utilities to expedite their repair process and can decrease downtime of this critical component. To address these issues of locating capacitor elements failures, this paper proposes an enhanced scheme for fault location detection in both grounded and ungrounded Y-Y SCBs; both for fuseless and internally fused units. Simulations of the proposed fault location method are carried out using PSCAD and MATLAB. The results validate the proposed method performance under pre-existing inherent unbalances, system voltage unbalance, and faults in the grid. The application and significance of the proposed method properties are demonstrated using illustrative simulation scenarios. This method can be integrated into a common unbalance protection of the multi-functional numerical capacitor bank relays and puts forth solutions to enhance fault location of SCBs. The method is capable of detecting consecutive capacitor elements failures, and also can mitigate gradual capacitance change due to temperature effects or natural aging. The presented fault location method is further enhanced to detect the number of failed elements.**

## I. Introduction

High Voltage (HV) Shunt Capacitor Banks (SCBs) are the most economical reactive power support components in power systems. Increasing the steady state transmittable power over transmission lines, and controlling the voltage profile at substations are examples of better utilization of power systems when SCBs are employed.

Present day HV SCBs are manufactured either using internally fused or fuseless capacitor unit designs. The fuseless units are cheaper; however, both of the technologies are advantageous to the externally fused designs. While identification of faulty capacitor units is simple with a blown external fuse, there is no visual indication for units with the other types, making their maintenance and fault investigation difficult and time consuming. Modern grids work close to their operation limits, and over-voltage duty is placed on transmission systems by today's load flow requirements. Utilities have also reported an increase in the frequency of failures in SCBs in recent years [1]. Integrating fault location algorithms into capacitor bank protective relays has become more vital with SCBs being more widely in use. Specifically, this is of importance for large (high voltage) SCBs, which have a wider search space in terms of the number of elements and units that comprise the bank. Locating the failed elements inside the SCBs is practically limited to detecting the phase to which the failed elements belong. This is adequate enough to narrow the search area and reduce the investigation time for locating the fault. In double wye SCBs with neutral current transformers (CT), this search area can be reduced by 83.3% because in this configuration each phase has two sections that are distinguishable in terms of failure location. As a result, the IEEE guide for protection of SCBs [2] recommends fault location logics as effective methods by which to speed up troubleshooting and repairing the banks.

A few recent publications provide information for locating the element failures inside the SCBs. In [3] a differential current measurement based approach is presented for fuseless SCBs that improves the protection selectivity for a bit more complex relaying algorithm requiring more CTs. In [4]–[6] an impedance measurement based approach has been presented that benefits from compensating temperature effects on impedance variation. Real time measured impedances are averaged to fine tune the nameplate values. This approach for fault location of fuseless SCBs includes measurement of all string currents. The basis of the rest of the fault location methods for SCBs is phase angle comparison, which is used to identify the phase in which the failed element is located [7], [8]. In [7]–[10] a method is introduced for faulted phase and section identification in ungrounded double wye SCBs. A fixed reference, e.g. positive sequence current for SCB with neutral current measurement, has been defined for the phase angle evaluation of a determined compensated quantity. The suggested method of these references neglects the negative sequence component of the current in deriving the expected value of the decision making function of fault location. In [11], a method which does not use neutral measurements is introduced. This primarily unbalance protection method uses compensated negative sequence current whose phase angle is compared with positive sequence voltage to detect the faulted phase. Having the present time measurements and

The major part of this paper has been accepted for publication in IEEE Transactions on Power Delivery, doi: 10.1109/TPWRD.2016.2583381

the commissioning time measurements, the pre-determined factor indirectly takes into account the temperature variations. This reference does not consider the shading effect. In [12] an algorithm for fault location is presented that relies on the comparison between consecutive measurements of the normalized unbalance current phase angle with respect to *one* of the phases. The compensation method in [12] for pre-existing unbalance and consecutive failures is based on determining step changes in the per-unitized neutral current. Detection of the number of failed elements is reported to be done by scaling the rms of neutral current to rms of a selected phase current (perunit) for a simulation gained look-up table. With regard to temperature impact and disturbances, in [12] it is claimed that by using the per unit value of the neutral current, it becomes independent of system transients and less dependent on the temperature changes.

The proposed fault location method of this paper can be integrated into the common unbalance protection of commercially available multi-functional numerical capacitor bank relays and puts forth solutions to enhance fault location of SCBs. The proposed method is devised with few simplifications to keep the fault location sensitive to the slightest failures, and includes assumption of inherent unbalance, due to manufacturing tolerances, for each phase and section of the SCB. Further, the presented algorithm is immune to instrument transformer errors, noise, harmonics, and external unbalances. Section II describes neutral current unbalance protection and its development for fault location. Section III explains the PSCAD and MATLAB simulation studies. Section IV presents the proposed method evaluation and comparison with conventional unbalance relaying. Finally, Section V concludes the results of the proposed method.

## II. Proposed Fault Location Algorithm

Unbalance protection methods use the evaluated unbalance for detection of abnormalities in a device and are the backbone of fault location. In these protection elements the known relationships among the measured voltages/currents taken around the SCB are used to indirectly monitor the changes in impedances. Neutral current unbalance protection (ANSI 60N) is selected for development of the proposed fault location method since this is the most common unbalance protection used for double wye banks. Also, this unbalance protection does not benefit from per phase unbalance quantity measurement, which makes it challenging in terms of fault location. It should be noted that in the equations in this paper the quantities: currents, k-factors, etc., represent vectors unless an absolute value sign is used.

### A. Ungrounded Double Wye SCB

Fig. 1 illustrates the circuit diagram and available measurements for an ungrounded double wye SCB with neutral current unbalance protection. Performing current division helps to relate the measured neutral current to phase currents

$$I_N = K_A I_A + K_B I_B + K_C I_C \tag{1}$$

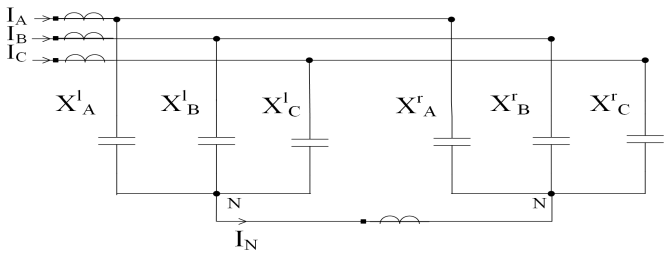


Fig. 1. Ungrounded double wye shunt capacitor bank.

where the phase coordinate k-factors when writing the neutral current in terms of the left section currents are defined as

$$K_p = \frac{X_p^r}{X_p^l + X_p^r} \qquad p : A, B \ \ or \ \ C \tag{2}$$

in which the phase impedances of the SCB are approximated as capacitive reactances [2] and the superscripts $r$ and $l$ denote the corresponding right section and left section reactances.
Assuming an element failure in the left section of phase A, that changes the left section reactance of this phase to $X_{Af}^l$, and thus yields to a new k-factor for phase A signified by $K_{Af}$. the neutral current changes to:

$$I_N = K_{Af} I_A + K_B I_B + K_C I_C \tag{3}$$

Subtracting (3) from (1) nulls out any pre-existing unbalance and makes the neutral current change caused by the internal failure stand out. The result is noted by compensated neutral current, $I_N^{Comp}$:

$$I_N^{Comp} = (K_{Af} - K_A) I_A \tag{4}$$

which evolves to

$$I_N^{Comp} = I_A X_A^r \frac{X_A^l - X_{Af}^l}{(X_A^l + X_A^r)(X_{Af}^l + X_A^r)} \tag{5}$$

Equation (5) signifies that for the faulted phase, depending on increase or decrease in the reactance, see (6), $I_N^{Comp}$ would be either in phase or out of phase with the corresponding phase current –location of the failure also affects the phase angle sign and will be discussed in (13) and (14).

$$\angle I_N^{Comp} = \angle I_A + \angle (X_A^l - X_{Af}^l) \tag{6}$$

$I_N^{Comp}$ should be expressed in terms of the measured current and adjustable setting. In this regard, the neutral current of (1) is re-written in terms of symmetrical components as it is common for the 60N operating function, see Appendix A, and ensures it is in accordance with the protection schemes of commercial relays [13].
As there is no path to the ground, $I_0$ is zero for ungrounded connections, and thus we have:

$$I_N = K_1 I_1 + K_2 I_2 \tag{7}$$

The two factors are complex conjugates of each other ($K_2 = K_1^*$), see Appendix A. In order to solve for the k-factors, the

following approach has been applied:
First (7) is multiplied by $I_1^*$

$$I_1^* \cdot I_N = I_1^* \cdot (K_1 I_1 + K_1{}^* I_2) \tag{8}$$

and then the conjugate of (7) is multiplied by $I_2$

$$I_2 \cdot I_N^* = I_2 \cdot (K_1{}^* I_1^* + K_1 I_2^*) \tag{9}$$

subtracting the results gives:

$$I_1^* \, I_N - I_2 \, I_N^* = K_1 \, |I_1|^2 - K_1 \, |I_2|^2 \tag{10}$$

therefore, we have:

$$K_1 = \frac{I_1^* \, I_N - I_2 \, I_N^*}{|I_1|^2 - |I_2|^2} \tag{11}$$

Equation (11) uses the measured currents to calculate the k-factors. To ensure the reliability of the unbalance k-factors, this calculation can be done using the average of several successive measurements of phase and neutral currents.
Since the final state for a failed element in internally fused banks is open circuit (operated fuse), and for fuseless banks short circuit, capacitive reactance of the affected phase will increase or decrease, respectively. To make the phase comparison adjustable for internally fused and fuseless banks, a sign factor, $K_{sg}$, is defined that expressed the final fault location principle, shown in (4), as

$$I_N^{Comp} = K_{sg} \, (I_N - (K_1 I_1 + K_2 I_2)) \tag{12}$$

Moreover, depending on whether the element has failed in the left section or right section of the SCB, (5) will get an additional negative sign. As a result, to make the decision boundary uniquely around $0^\circ$ phase angle difference, between $I_N^{Comp}$ and the faulted phase current, $K_{sg}$ is defined as follows. For fuseless SCBs:

$$K_{sg} = \begin{cases} +1 & \text{Left Section Evaluation} \\ -1 & \text{Right Section Evaluation} \end{cases} \tag{13}$$

For internally fused SCBs:

$$K_{sg} = \begin{cases} -1 & \text{Left Section Evaluation} \\ +1 & \text{Right Section Evaluation} \end{cases} \tag{14}$$

*1) Detection of the number of failed elements:* The consequence of an element failure in one of the sections is the change in the reactance value. The effect on the neutral current magnitude should therefore be evaluated to set a reference for fault location application. Typical sensitivity analysis for 60N [13] is adapted to suit the proposed fault location scheme for this purpose. It is worth noting that, as in the common design for double wye ungrounded SCBs, the left and right section of the bank may not have the same reactance, and so the reference value for detection of the number of failed elements should be set separately for each section. To find the change in the neutral current with development of a single element failure in the left section, a failure is assumed in one of the phases, say phase A. With reference to (1) and (2), the derivative of the neutral current can be used to derive the required setting:

$$\frac{d\,I_N}{dX_A^l} = \frac{d(K_A I_A + K_B I_B + K_C I_C)}{dX_A^l} = \frac{dK_A}{dX_A^l} \, I_A \tag{15}$$

which gives the following identity

$$\frac{d\,I_N}{dX_A^l} = \frac{-X_A^r}{(X_A^l + X_A^r)^2} \, I_A \tag{16}$$

Similarly, for a failure in the right section of phase A, one can derive:

$$\frac{d\,I_N}{dX_A^r} = \frac{X_A^l}{(X_A^l + X_A^r)^2} \, I_A \tag{17}$$

Similar equations hold true for phase B and C. To form a setting from the derived equations, the phase current is replaced by the rated current of the SCB, $I_r$, and the absolute value of the differentials is presented in terms of changes. Both the change in reactance and the change in neutral current are expressed in perunit values. Assuming that the following relationship exists between the left section and the right section perphase reactances:

$$X^r = K_x \, X^l \tag{18}$$

The base value for neutral current changes would become:

$$\Delta\, I_N(\text{pu}) = \begin{cases} \Delta X_A^l(\text{pu}) \times \frac{K_x}{(K_x+1)^2} & \text{Left section setting} \\ \Delta X_A^r(\text{pu}) \times \frac{1}{(K_x+1)^2} & \text{Right section setting} \end{cases} \tag{19}$$

where left section reactance is selected as the base for reactance change and the rated phase current as a base for neutral current change.
$\Delta\, X(\text{pu})$ is calculated for a single element failure, hence the $\Delta\, I_N(\text{pu})$ will form a base for detection of number of failed elements that is also used to set a magnitude threshold for triggering the phase comparison. Details on application settings and how the setting quantities are calculated for a given SCB are provided in Appendix B.

### *B. Grounded Double Wye SCB*

Fig. 2 shows a double wye grounded SCB with neutral current unbalance protection. As there is a path to the ground in this configuration, the zero sequence current exists in the neutral current. However, even sensitive unbalance protection methods [14] have to ignore the effect of zero sequence current. This is because compensating the pre-existing unbalance caused by all three sequences of current, i.e. setting three k-factors, requires a set of three equations while we always have just a set of two (real and imaginary parts of the neutral current). As a result, the zero sequence current is left uncompensated [2]. Such an assumption does not render loss of reliability for the protection and fault location. The reason is, first, the two sections of these grounded banks are manufactured to be identical in impedance (factory matched). Second, a window CT measuring the vectorial difference between the neutral currents is applied. Although for protection

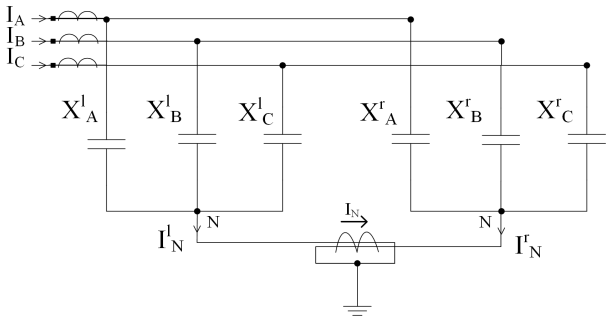


Fig. 2. Grounded double wye shunt capacitor bank.

a percent restraint supervision is applied [13], results show that fault location is secure without the restraint. See Section IV and Appendix A for results and more details.

Using the circuit diagram of Fig. 2 and similar to the way the neutral current was derived for ungrounded SCBs, subtracting the left and right sum of section currents leads to the following identity

$$I_N = I_N^l - I_N^r = (K_A^l - K_A^r)I_A + (K_B^l - K_B^r)I_B + (K_C^l - K_C^r)I_C = K_A I_A + K_B I_B + K_C I_C \quad (20)$$

where the phase coordinate k-factors are

$$K_p = \frac{X_p^r - X_p^l}{X_p^l + X_p^r} \qquad p : A, B \ \ or \ \ C \quad (21)$$

The same transformation to sequence components, and k-factor calculations of ungrounded SCBs applies to grounded ones. The compensated neutral current and the sign factors for fuseless and internally fused SCBs are the same as (12), (13), (14), respectively.

*1) Detection of number of failed elements:* The same approach as the one presented for ungrounded SCBs is applied for grounded ones. The only difference that affects the final setting is the identity that relates the value of the phase coordinate k-factors to the phase reactances per (21). For grounded SCBs, the two sections are factory matched, which means the base for the number of failed elements would be the same for both. The derivation is expressed as

$$\frac{d\,I_N}{dX_A^l} = \frac{d(K_A I_A + K_B I_B + K_C I_C)}{dX_A^l} = \frac{dK_A}{dX_A^l} I_A = \frac{d(\frac{X_A^r - X_A^l}{X_A^l + X_A^r})}{dX_A^l} I_A = \frac{-2X_A^r}{(X_A^l + X_A^r)^2} I_A \quad (22)$$

Taking the same procedure for a failure in the right section will give the same result but with the opposite effect on the magnitude of the neutral current due to the differential property of the measured current through the window CT at the neutral. The expected values for $X_A^r$ and $X_A^l$ are the same for this configuration, denoting both of them as $X$ and expressing the values in perunit, the same as what was done for ungrounded SCBs, gives the base value for number of failed elements detection as

$$\Delta\, I_N(\text{pu}) = \frac{\Delta X}{2}(\text{pu}) \quad (23)$$

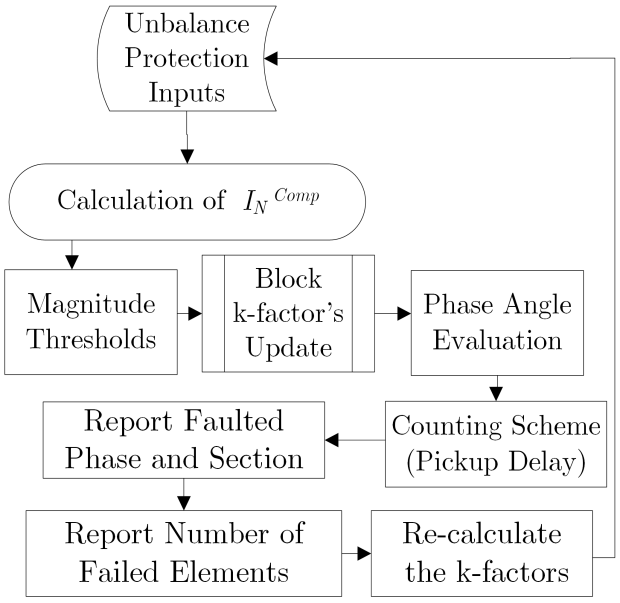


Fig. 3. Proposed algorithm flowchart for internal failure investigation.

### C. Considerations for Temperature Effects on Reactance

There is considerable temperature variance when substation equipment is either in the shade or under direct sunlight. Partial shading is also expected when part of the bank is under shadow and the rest under sunlight [15]. Assume a maximum ambient temperature of $55°$C for a SCB in operation [16], then for an extreme temperature difference of say $30°$C, the change in capacitance of a power capacitor could reach $1.5\%$, based on [3]. This happens over an interval of several hours. By comparison, according to (B.3) and (B.4), an element failure causes around $0.3\%$ change in the capacitance within a few milliseconds. Therefore, it takes thousands of seconds for a shading effect to be able to mimic such a change. The conclusion is that updating the k-factors once or twice an hour is enough to keep the fault location sensitive and secure. To avoid interference with the fault location, this regular updating should be blocked for a short while, once an internal failure is suspected, i.e. the phase angle comparison is triggered. In fact, a combination of self-tuning and auto-setting [14] is applied in the proposed method.

### D. Flowchart of the Proposed Fault Location Method

Fig. 3 illustrates the flowchart of the proposed method. In this section we will go through the parts of the flowchart that have not been explained in the previous sections.

The last set of k-factors will be used for the calculation of $I_N^{Comp}$ based on (12). Upon passing a pre-determined magnitude threshold, the phase comparison will be triggered. With reference to (5), this comparison implies that phase angle

difference of (12) with phasor of the current of the faulted phase should approach and stay in a defined boundary around zero. The boundary is applied to increase the reliability of the fault location and is chosen to be $15^\circ$ [10]. The counting scheme implies that for each and every execution of the fault location algorithm, when both magnitude and phase comparisons satisfy their criteria, there would be a count up until this reaches a certain number, and if any of them do not fulfill their conditions a countdown will be performed. The counting threshold, pick up delay, can be set to say 100 ms and would able to detect consecutive failures that are as close as say 200 ms to each other.

## III. Simulation Model

### A. Relay Model Description

Fourth order butter-worth anti-aliasing filters with a cut off frequency of 1536 Hz are applied to the outputs of the CT models. Sampled phase and neutral currents are recorded and played back in MATLAB for the relay model. The relay model includes a decaying DC removal filter and uses full cycle Discrete Fourier Transform (DFT) for phasor estimation. Phasor estimation and fault location algorithm can be executed 8 times per power frequency cycle.

### B. Simulated System and Capacitor Bank Configurations

A simple power system is modeled in PSCAD as shown in Fig. 5. Harmonic currents have been injected to create voltage distortions according to the limits set by IEEE standard 519 [17]. Signal to Noise Ratio (SNR) of the output of current transformers are assumed to be 50 dB based on their rated secondary current. This guarantees reliable operation for even lower SNRs, because for the neutral CT the actual current is far less than the rated secondary value.

For evaluations under unbalanced voltages, an unbalanced load is employed. Transmission level voltage unbalance of around 2% [18] is considered using the percentage Voltage Unbalance Factor (%VUF) definition in [19]:

$$\%VUF = \frac{V_2}{V_1} \times 100 \tag{24}$$

Regarding pre-existing phase reactance unbalance, the requirement is reported to be about 1% [1]. To validate algorithm performance, this maximum allowable inherent unbalance is simulated.

Neutral current waveform of a sample scenario in which a single element fails in one of the six possible locations is selected to show the effectiveness of the anti-aliasing and the applied DFT filter, results are shown in Fig. 4. Note that the uncompensated neutral current is depicted in this figure, i.e. besides the noise and harmonics, the signal also carries the system unbalance and pre-existing inherent unbalance of the bank. The algorithm has been validated to be robust and accurate in estimating the fundamental frequency phasor in presence of noise. As we are dealing with internal failures in the SCBs, the modeled bank configurations and unit constructions are provided in more detail. Figs. 6 and 7 illustrate both the bank

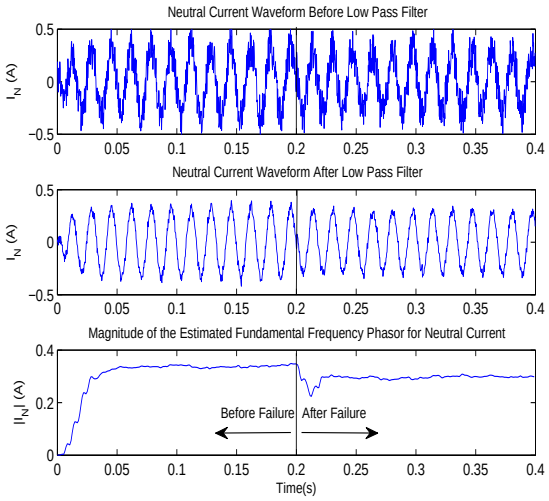


Fig. 4. Low pass filter and DFT filter application on the measured signal.

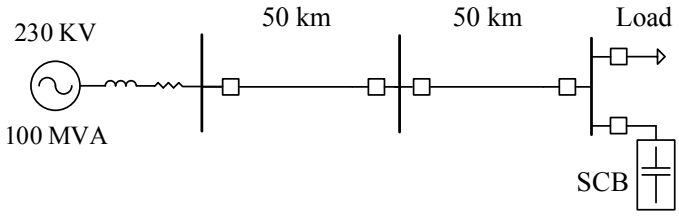


Fig. 5. Modeled power system in PSCAD.

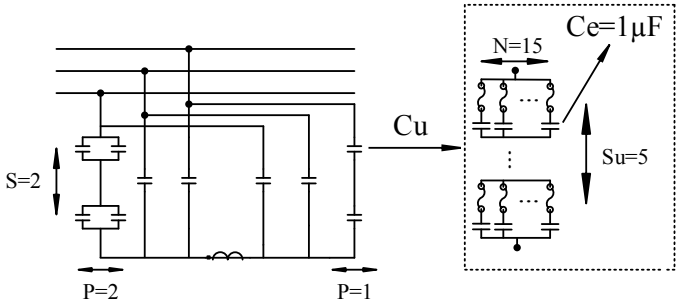


Fig. 6. Modeled 230 kV internally fused ungrounded double wye SCB with single string per phase for each section.

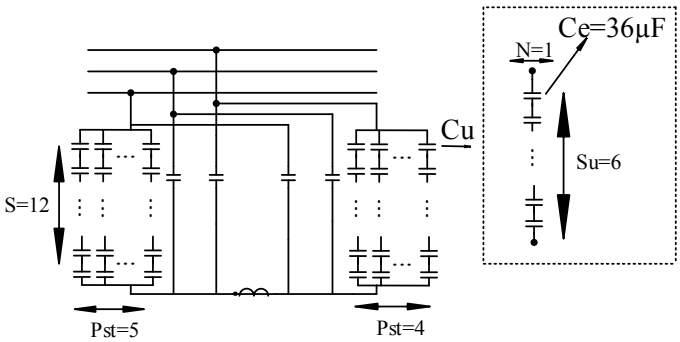


Fig. 7. Modeled 230 kV fuseless ungrounded double wye SCB.

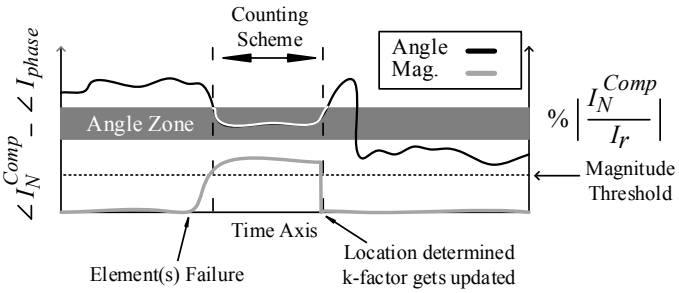


Fig. 8. Figure interpretation guide.

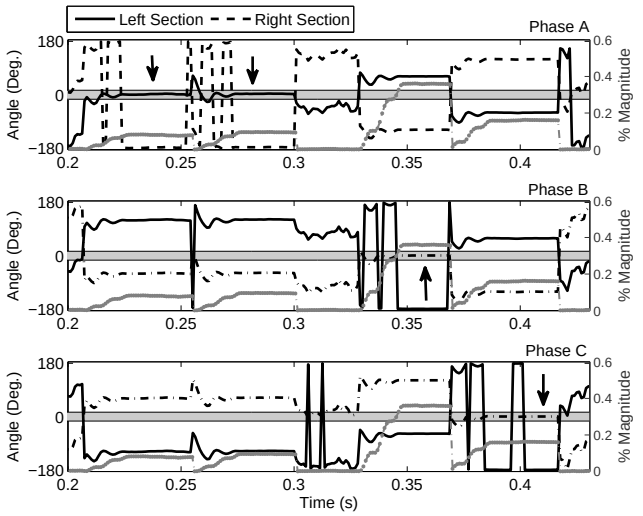


Fig. 9. The proposed method evaluation for an ungrounded SCB.

and unit construction for ungrounded double wye SCBs. The series/parallel connection of units and the construction of each unit for grounded banks is identical for left and right sections. The internally fused grounded SCB was modeled having both sections the same as the left section of the SCB in Fig. 6, and the fuseless grounded SCB was modeled having both sections the same as the left section of the SCB in Fig. 7.

## IV. Proposed Method Evaluation

Various internal failure scenarios were simulated and the performance of the proposed method for reliable determination of their location and estimation of the number of failed elements was evaluated under different conditions, including different external unbalances. Here selected illustrative examples are presented to demonstrate the validation.

Fig. 8 demonstrates a guide for the evaluation figures. The phasor magnitude of the principle defined in (12) and its referenced phase angle are plotted, in black and gray, respectively. As per (5), for fault location, the principle's phase angle is referenced to the phase angle of the three phase current phasors. In the evaluation figures, these are plotted separately to increase the clarity of the figures. In Fig. 8, it is shown that, with the failure of the elements inside the bank, the magnitude of the principle reaches the estimated value, which corresponds to the number of failed elements. The referenced phase angle for the faulted phase also reaches the angle zone (around zero degrees). The magnitude and angle will stay in their related boundaries unless we reset them by updating the k-factors. This is done once the counter reaches its threshold and helps to detect subsequent failures. The intervals that have led to resetting the principle will be identified with arrows in the evaluation figures.

### A. First Failure

Fig. 9 illustrates the proposed method's principle variation for a simulation scenario as reported by Fig. 10. Results are shown for a fused SCB. The first failure happens in the left section of phase A at 0.2 s. The magnitude of the compensated neutral current in percentage of rated current goes beyond the threshold and at the same time the referenced phase angle falls into the angle boundary of zero for phase A. Thus, the fault location is determined, and according to the magnitude value with respect to the setting, derived per (19), a single element failure is reported in Fig. 10. A similar scenario happens for phase C right section at 0.36 s and is detected and reported accordingly.

### B. Consecutive Failure

After the first failure is detected, the k-factors were reset and thus the algorithm is ready to detect a consecutive failure. In this illustrative example, the consecutive failure happens at 0.25 s. As can be seen in Fig. 10, the consecutive failure is also detected and adds to the number of failed elements in the corresponding section of phase A.

### C. Multiple Element Failure

Two elements fail in the right section of phase B at 0.32 s, simultaneously. The same detection procedure applies with the difference that the fault location principle magnitude change from the reset (zero) value is twice the base setting. The number of failed elements is also reported accordingly.

### D. On Ambiguous Failures

As can be seen with the latching option and auto-update of the k-factors no ambiguous failure can affect the outputs of the proposed method. The principle is reset in order that the past failures do not affect detection of subsequent failures, and each failure is detected and reported separately while the state of the SCB is stored.

### E. Susceptibility to External Disturbances

Fig. 11 shows the proposed method's principle variation for a scenario in which a phase A to ground fault takes place at the SCB bus at 0.2 s. The fault is cleared at 0.3 s, and meanwhile an internal failure in the right section of phase A is simulated at 0.22 s. Two elements fail in the left section of phase C at 0.36 s, then a single phase tripping takes place in phase C of the connecting transmission line at 0.38 s and a successful reclosure happens at 0.48 s. The short deadtime for single phase auto-reclosure has been assumed for the sake of

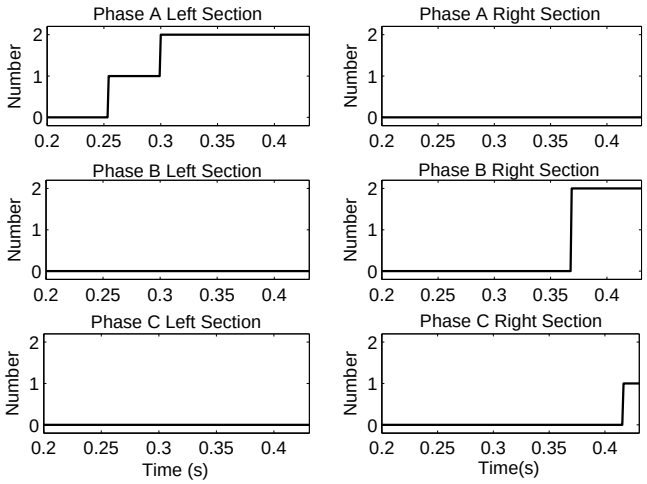


Fig. 10. Detected location and number of failed elements for ungrounded SCB.

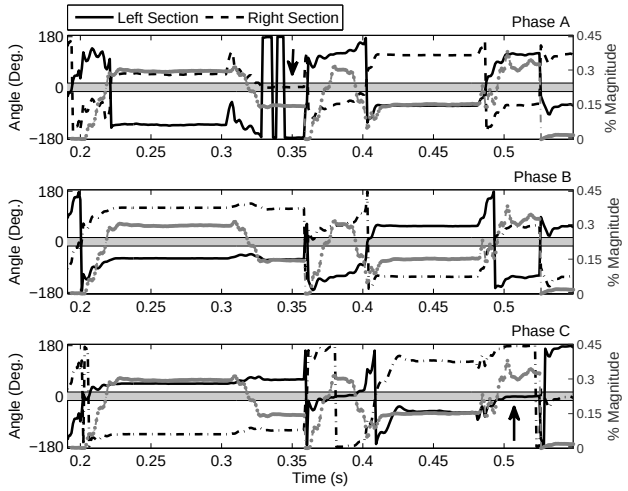


Fig. 11. The proposed method evaluation for a grounded SCB.

clarity of the demonstration. Results are shown for a fuseless SCB. As can be seen in the fault location report, presented in Fig. 12, the external failures do not render spurious reports, although they introduce detection delays.

With regard to transient overvoltage of energizing or possible restrike on de-energizing, commercial unbalance protection elements have intentional delays in order not to operate during these transients. Blocking signals can be assigned from breaker monitoring and capacitor control elements to further support the security of supervised functions, such as fault location. In addition, similar to the presented illustrative scenarios for external faults, the fault location would be able to determine the failure once the transients totally vanish. This holds true unless, in the short interval of these transients, element failures occur in more than one of the six possible locations.

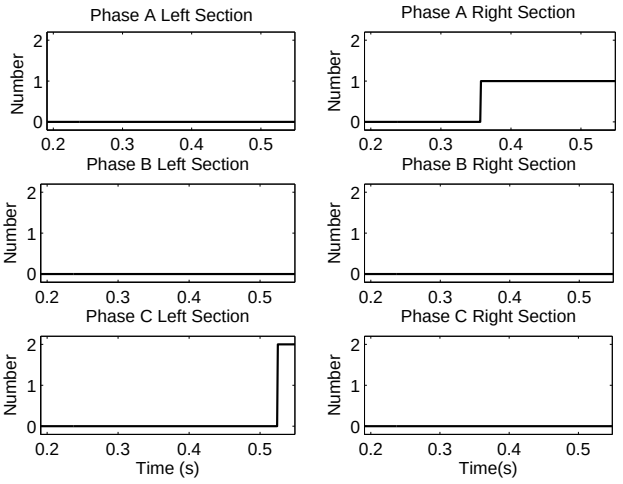


Fig. 12. Detected location and number of failed elements for grounded SCB.

### *F. Compensation for Gradual Reactance Changes*

To demonstrate the importance of the regular updating of the k-factors and how it mitigates the effect of gradual changes in reactance caused by weather conditions, partial shading or aging, an illustrative simulation is performed. A linear change in the capacitance of the left section of phase A of a fused ungrounded SCB is assumed. The change starts at 0.2 s and its upward ramp ends after about 50 ms. Algorithm setting for regular updates is set faster than the linear change rate and triggers once every fifteen protection passes (an arbitrary setting for this illustrative example). As a worst case scenario, it is assumed that the other phases and sections of the SCB do not experience the linear capacitance change so that the event can exactly mimic an internal failure. Note that for the sake of simplicity and clarity of the plot, the rate of change is much faster than what we explained in Section II-C. Fig. 13 presents the fault location principle variations. The moments of regular reset are signified by arrows. As can be seen, without a regular update, such a condition can lead to a false failure report as both magnitude and angle criterion can satisfy the fault location conditions.

### *G. Importance of Considering Negative Sequence Component Impact on the Fault Location Phase Comparison*

To demonstrate the point in considering the impact of phase angle of negative sequence current on the angle comparison part of the algorithm, the proposed fault location code is re-written with an assumption that the phase current in (6) constitutes only positive sequence current for an ungrounded SCB. The illustrative scenario takes place with an internal failure in the left section of phase A of a fuseless SCB at 0.2 s and occurrence of a single phase tripping in phase B at the same time, which is reclosed at 0.3 s. Figs. 14 and 15 show the principle variations for the proposed method and the modified code, respectively. As can be observed, without considering the negative sequence phase angle impact, the

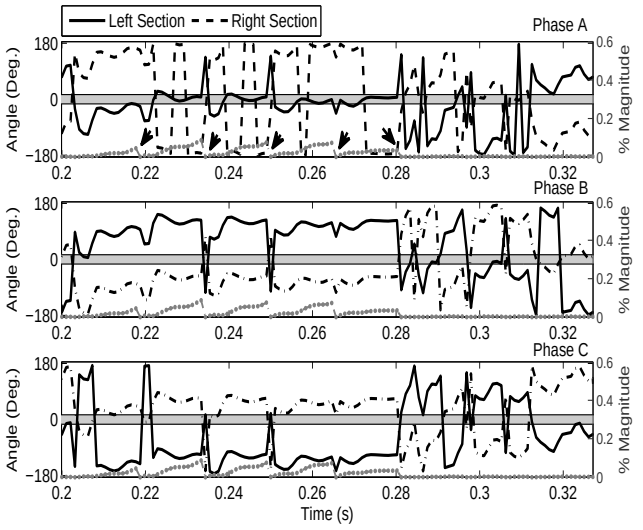


Fig. 13. Impact of regular updates of the k-factor on security of the proposed fault location method.

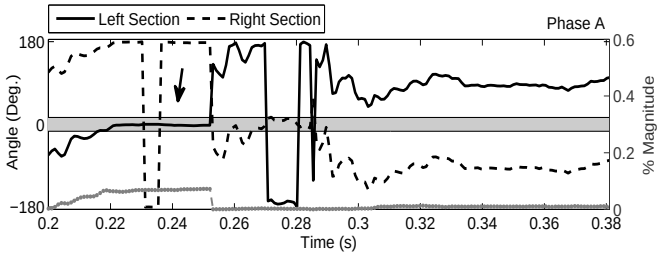


Fig. 14. The proposed method evaluation for external unbalance (negative sequence phase angle impact is considered).

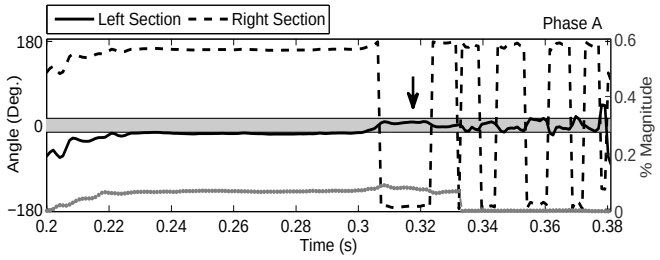


Fig. 15. The modified proposed method evaluation for external unbalance (negative sequence phase angle impact is neglected).

delay in detecting and locating the failure is much longer. Considering the fact that the modified code can only detect the failure after clearance of the external event, which could last for a second in the case of single phase auto reclosure, the delay would be of particular importance as the greater delay a fault location method has, the higher the likelihood of missing consecutive failures. It is worthwhile to note that occurrence of cascading failures has a higher possibility while an external unbalance exists in the system as it can put more voltage stress on the elements.

### *H. Method Advantages to Conventional Unbalance Relaying Alarms*

To test the neutral current unbalance protection for comparison with the proposed faulted phase and section detection method, the following illustrative scenario was selected:

- Single element failure in phase B left section, at 0.2
- Consecutive failure in phase B right section, at 0.25
- Single element failure in phase C left section, at 0.3
- Consecutive failure in phase C right section, at 0.35

Figure 16 shows successful monitoring of all of the four failures by the proposed method. Figure 17 depicts the resultant outputs from the proposed fault location method.

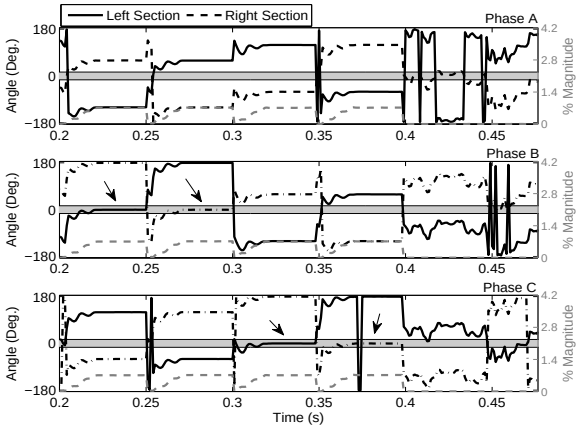


Fig. 16. Faulted Phase and Section Determination, Decision Criteria.

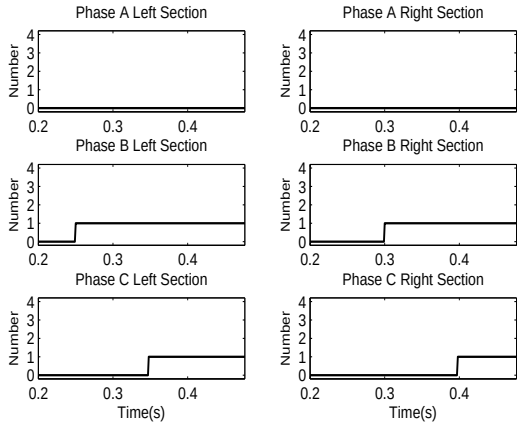


Fig. 17. Faulted Phase and Section Determination, Outputs.

The COMTRADE records were played back for a commercial capacitor bank protection and control relay. After adjusting each stage's pick up value the following points can be seen in the resultant relay oscillography records, see Figure 18, where the top plot shows the operating quantity which is magnitude of a neutral current based signal.

- At instant 1, STG 1 has picked up, however the faulted phase is unknown.

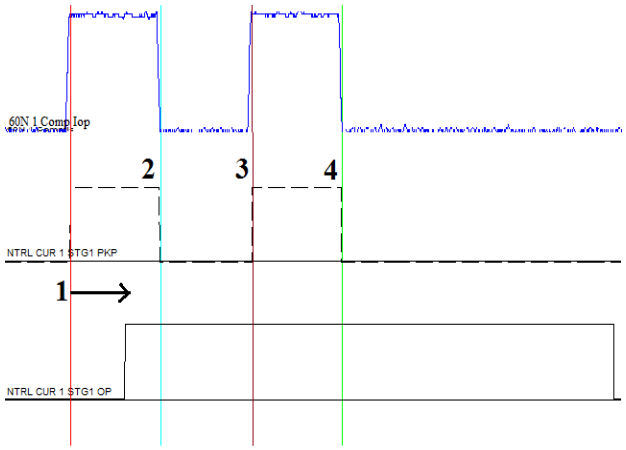


Fig. 18. Relay oscillography records for neutral current unbalance protection.

- At instant 2, the offsetting effect resets the operating quantity (ambiguous failure), the consecutive failure is missed and even the previous failure is determinable only when the drop out delay is high or operand has a latched setting.
- At instant 3, again STG 1 picks up but without faulted phase information.
- At instant 4, again offsetting resets the operating quantity resulting in missing the events.

## V. Conclusion

A comprehensive investigation on fault location in double wye shunt capacitor banks with neutral unbalance protection was performed. The investigation covers both ungrounded and grounded banks with either of the internally fused or fuseless technologies. To improve the outcome of the existing methods, the proposed method applies dynamic unbalance compensation and self-tuning for detecting consecutive failures and negating the capacitive reactance gradual changes due to temperature changes and aging. Detection of the number of failed elements is also an enhancement that was applied to the fault location. For double wye shunt capacitor banks, system (external) unbalance affects both wye sections equally, so there is no need to block the fault location under such a condition. Accordingly, the proposed method performs well in the presence of external unbalances and disturbances so there is low chance of not detecting internal capacitor failures. The results verify the reliability of the proposed method considering measurement noise, harmonics, bank inherent unbalance, and system unbalance. Required data for application settings was also provided.

## VI. References

[1] M. Ellis, D. Meisner, and M. Thakur, "Innovative protection schemes for h configuration fuseless grounded shunt capacitor banks," in *Protective Relay Engineers, 2012 65th Annual Conference for*, April 2012, pp. 449–458.

[2] "IEEE Guide for the Protection of Shunt Capacitor Banks," *IEEE Std C37.99-2012 (Revision of IEEE Std C37.99-2000)*, pp. 1–151, March 2013.

[3] E. Price and R. Wolsey, "String current unbalance protection and faulted string identification for grounded-wye fuseless capacitor banks," in *65th Annual Georgia Tech Protective Relaying Conference*, May 2011.

[4] T. R. Day and D. P. Roth, "Device protection using temperature compensation," US Patent 7 990 668, August, 2011.

[5] L. Fendrick, T. Day, K. Fender, J. McCall, and A. Chaudhary, "Complete relay protection of multi-string fuseless capacitor banks," in *Pulp and Paper Industry Technical Conference, 2002. Conference Record of the 2002 Annual*, June 2002, pp. 194–198.

[6] A. Chaudhary, T. Day, K. Fender, L. Fendrick, and J. McCall, "Pull a few strings [complete protection of multistring fuseless capacitor banks]," *Industry Applications Magazine, IEEE*, vol. 9, no. 6, pp. 34–39, Nov 2003.

[7] S. Samineni, C. Labuschagne, and J. Pope, "Principles of shunt capacitor bank application and protection," in *Protective Relay Engineers, 2010 63rd Annual Conference for*, March 2010, pp. 1–14.

[8] S. Samineni, C. Labuschagne, J. Pope, and B. Kasztenny, "Fault location in shunt capacitor banks," in *Developments in Power System Protection (DPSP 2010). Managing the Change, 10th IET International Conference on*, March 2010, pp. 1–5.

[9] S. Samineni and C. A. Labuschagne, "Apparatus and method for identifying a faulted phase in a shunt capacitor bank," US Patent 8 575 941, November, 2013.

[10] J. Schaefer, S. Samineni, C. Labuschagne, S. Chase, and D. Hawaz, "Minimizing capacitor bank outage time through fault location," in *Protective Relay Engineers, 2014 67th Annual Conference for*, March 2014, pp. 72–83.

[11] A. Kalyuzhny, J. C. Mccall, and T. R. Day, "Corrective device protection," US Patent 7 973 537, July, 2011.

[12] Z. Gajic, M. Ibrahim, and J. Wang, "Method and arrangement for an internal failure detection in a y-y connected capacitor bank," US Patent 20 130 328 569, December, 2013.

[13] *C70 Capacitor Bank Protection and Control System, UR Series Instruction Manual, Section 9.1.6*, GE Digital Energy, November 2014.

[14] B. Kasztenny, D. McGinn, and I. Voloh, "Enhanced adaptive protection method for capacitor banks," in *Developments in Power System Protection, 2008. DPSP 2008. IET 9th International Conference on*, March 2008, pp. 269–274.

[15] R. Moxley, J. Pope, and J. Allen, "Capacitor bank protection for simple and complex configurations," in *Protective Relay Engineers, 2012 65th Annual Conference for*, April 2012, pp. 436–441.

[16] "IEEE Standard for Shunt Power Capacitors," *IEEE Std*

*18-2012 (Revision of IEEE Std 18-2002)*, pp. 1–39, Feb 2013.

[17] "IEEE Recommended Practice and Requirements for Harmonic Control in Electric Power Systems," *IEEE Std 519-2014 (Revision of IEEE Std 519-1992)*, pp. 1–29, June 2014.

[18] *Review of Voltage Unbalance Limit in The GB Grid Code CC.6.1.5 (b)*, NationalGrid, Oct. 2014.

[19] P. Pillay and M. Manyage, "Definitions of voltage unbalance," *Power Engineering Review, IEEE*, vol. 21, no. 5, pp. 49–51, May 2001.

[20] B. Kasztenny, J. Schaefer, and E. Clark, "Fundamentals of adaptive protection of large capacitor banks - accurate methods for canceling inherent bank unbalances," in *Protective Relay Engineers, 2007. 60th Annual Conference for*, March 2007, pp. 126–157.

## VII. Biographies

**Hessamoddin Jouybari-Moghaddam** received the M.Sc. degree in electrical engineering from Amirkabir University of Technology, Tehran, Iran, in 2012, and is currently pursuing the Ph.D. degree in electrical and computer engineering at the University of Western Ontario (Western University), London, ON, Canada. His research interests include power system protection, monitoring, and automation.

**Tarlochan Sidhu** (M'90-SM'94-F'04) received the Ph.D. degree in electrical engineering from University of Saskatchewan, Saskatchewan, Saskatoon, SK, Canada, in 1989. He is currently a Professor and Dean of Faculty of Engineering and Applied Science at University of Ontario Institute of Technology (UOIT), Oshawa, ON, Canada. Prior to this, he was a Professor and Chair of the Electrical and Computer Engineering Department at the University of Western Ontario, London, ON, Canada. He also has held the NSERC/Hydro One Senior Industrial Research Chair in Power Systems Engineering. His research interests include power system protection, monitoring, control and automation.

**Palak Parikh** (M'11) received B.Sc. and M.Sc. degrees in electrical engineering from Sardar Patel University, India, in 2003 and 2005, respectively and the Ph.D. degree in electrical and computer engineering from University of Western Ontario, London, ON, Canada in 2011.

She is currently working with GE Grid Solutions in product R&D application engineering group. Palak has expertise in the area of power protection, distribution automation & microgrid solutions. She is author of more than 16 international journal and conference articles.

**Ilia Voloh** (M'99, SM'03) received his Electrical Engineering degree from Ivanovo State Power University, Russia. He is currently consulting engineer-protection with GE Grid Solutions, Markham, ON, Canada. His areas of interest are advanced power system protection algorithms and advanced communications for protective relaying. Ilia authored and co-authored more than 40 papers presented at major North America Protective Relaying conferences. He is a member of IEC TC95 committee, active member of the main IEEE PSRC committee and a senior member of the IEEE.

## Appendix A
## Proof of Complex Conjugate k-factors

It is typical in 60N operating signal developments to write (1) in terms of symmetrical components [2], [14]; knowing this, the resultant equation would be

$$\begin{aligned} &I_N = K_A(I_1 + I_2 + I_0) + K_B(a^2 I_1 + aI_2 + I_0) \\ &+K_C(aI_1 + a^2 I_2 + I_0) = I_1(K_A + a^2 K_B + aK_C) \\ &+I_2(K_A + aK_B + a^2 K_C) + I_0(K_A + K_B + K_C) \end{aligned} \quad (A.1)$$

where $a = e^{j\frac{2\pi}{3}}$.

For ungrounded SCBs the last term is actually equal to zero. For grounded SCBs the coefficient of $I_0$ in (A. 1) itself is likely to have a very small value as the k-factors of different phases defined by (21) might be of varying signs. Therefore, the last term in (A. 1) is usually neglected [13] which results in (A. 2). It is worth noting that in some references even the negative sequence term is also neglected [20].

$$\begin{aligned} I_N &\simeq I_1(K_A + a^2 K_B + aK_C) + I_2(K_A + aK_B + a^2 K_C) \\ &= K_1 I_1 + K_1^* I_2 \end{aligned} \quad (A.2)$$

Since $K_{A,B,C}$ are real values and $a^2 = a^*$, the two k-factors are proved to be complex conjugates of each other.

## Appendix B
## Required Data for Application Settings

| | |
|---|---|
| Su | No. of Series groups in the unit |
| N | No. of Parallel elements in a group |
| P | No. of Parallel units in a group |
| Pst | No. of Parallel strings per phase |
| S | No. of Series groups, line to neutral |
| Qu | Rated kVAR of each unit |
| Vu | Rated voltage of each unit (kV) |
| Q | Rated MVAR of the SCB (three phase) |
| V | Rated line to line voltage of the SCB (kV) |
| Ce | Element capacitance ($\mu$F) |
| Cu | Unit capacitance ($\mu$F) |

The required data for the fault location algorithm is summarized in this section, which also explains how capacitor and unit construction information is used for setting calculations. Where the element capacitance is not provided directly, capacitance of each element can be calculated using the ratings and construction information of each capacitor unit, see (B. 1).

$$Ce = Cu \times \frac{Su}{N} = \frac{Su \times Qu}{N \times Vu^2 \times \omega} \times 10^3 \ (\mu F) \quad (B.1)$$

where $\omega$ denotes angular frequency in $rad/s$. Based on the provided construction information for both the bank and its units, the after failure and before failure capacitance are calculated by the fault location algorithm considering a single element failure. Rated primary per phase current of the SCB is also calculated as follows:

$$I_r = \frac{Q}{\sqrt{3}V} \times 10^{-3} \quad (A) \quad (B.2)$$

The before failure per phase capacitance is derived as

$$C = Cu \times \frac{P \times Pst}{S} \tag{B.3}$$

For fuseless banks, according to definition [13], $P$ equals unity. The after failure per phase capacitance would be

$$\frac{Cu \times P}{S}(Pst-1)+\frac{Cu \times P}{S-1} \parallel (C_{uf}+(P-1)\times Cu) \tag{B.4}$$

where $C_{uf}$ denotes the after single element failure capacitance of the unit. Depending on the fusing method, this capacitance will have one of the following values

$$C_{uf} = \frac{Ce \times N}{Su-1} \qquad \text{Fuseless Bank} \tag{B.5}$$

$$C_{uf} = (\frac{Ce \times N}{Su-1}) \parallel (Ce \times (N-1)) \qquad \text{Fused Bank} \tag{B.6}$$

where the operator $\parallel$, implies the following identity:

$$C_1 \parallel C_2 = (\frac{1}{C_1}+\frac{1}{C_2})^{-1} \tag{B.7}$$

These equations apply for each section of the double wye bank. The corresponding capacitive reactances are calculated where needed as $X = \frac{1}{C\omega}$.